Hindawi
Journal of Nanomaterials
Volume 2017, Article ID 9248153, 7 pages
https://doi.org/10.1155/2017/9248153

Research Article

C_{60} Filling Rate in Carbon Peapods: A Nonresonant Raman Spectra Analysis

Fatima Fergani,[1] Sidi Abdelmajid Ait Abdelkader,[1] Hassane Chadli,[1] Brahim Fakrach,[1] Abdelhai Rahmani,[1] Patrick Hermet,[2] and Abdelali Rahmani[1]

[1]*Laboratoire d'Etude des Matériaux Avancés et Applications (LEM2A), Université Moulay Ismaïl, FSM-ESTM, BP 11201, Zitoune, Meknes, Morocco*
[2]*Institut Charles Gerhardt Montpellier, UMR-5253, CNRS, Université de Montpellier, ENSCM, Place E. Bataillon, 34095 Montpellier, France*

Correspondence should be addressed to Abdelali Rahmani; a.rahmani@fs-umi.ac.ma

Received 31 January 2017; Accepted 19 April 2017; Published 18 May 2017

Academic Editor: Paulo Cesar Morais

We calculated the nonresonant Raman spectra of C_{60} peapods to determine the concentration of C_{60} fullerenes inside single-walled carbon nanotubes. We focus on peapods with large diameters for which C_{60} molecules can adopt a double helix configuration or a two-molecule layer configuration. Our calculations are performed within the framework of the bond-polarizability model combined with the spectral moment's method. The changes in the Raman spectra as a function of C_{60} filling rate and the configuration of C_{60} molecules inside the nanotubes are identified and discussed. Our calculations support the experimental method proposed by Kuzmany to evaluate the concentration of C_{60} molecules inside nanotubes.

1. Introduction

Single walled carbon nanotubes (SWCNT) can encapsulate small and large molecules such as fullerenes [1–5]. A C_{60} peapod consists of a SWCNT in which C_{60} fullerene molecules are inserted. This hybrid system between C_{60} fullerene and SWCNT has generated a lot of interest for future electronic applications. Carbon peapods have been proposed as possible candidates for novel nanometer scale devices and many efforts are devoted to the synthesis of high-quality 1D fullerene crystals inside SWCNTs [1, 4]. Due to their original one-dimensional nanosized structure and their tunable electronic properties, peapods have several potential applications as high temperature superconductors [6], memory elements [7], and nanometer-sized containers for chemical reactions [3].

The structure of C_{60} fullerenes inside SWCNTs is strongly dependent on the nanotube diameter, so that even small changes in the SWCNT diameter can alter the geometry of fullerene arrays. From an experimental point of view, structural analysis of peapods can be performed using transmission electron microscopy [1, 4], electron diffraction [5, 8], X-ray scattering [9], and/or Raman spectroscopy [4, 9, 10]. From a theoretical point of view, the organization of fullerenes inside nanotubes has been studied using several models: energy calculations with a simple van der Waals potential [11, 12], Monte Carlo, and molecular dynamic based methods [13–15]. It was shown that C_{60} molecules inside SWCNTs with a wide range of diameters (1.25–2.71 nm) can form ten different packing arrangements [13, 14]. According to the theoretical calculations, C_{60} molecules can arrange in a chiral array inside the SWCNTs although such a double helical packing arrangement appears to be less prominent than the zigzag one. Nevertheless, Khlobystov et al. [16] observed the double helical array of C_{60} molecules inside a SWCNT and a two-molecule layer inside a double-walled carbon nanotube (DWCNT) by high-resolution TEM. The helix formation of encapsulated C_{60}'s corresponds to a weaker binding, which was shown to lead to a reversible filling-removal process of the fullerenes [17]. C_{60} encapsulation was successfully used as a starting point for in-the-tube chemistry [18] and because of the experimental stimuli, the enclosed

C_{60} peas transform into SWCNTs within the outer tubes, thus producing double-wall carbon nanotubes [19].

Raman spectroscopy is one of the promising tools to characterize carbon nanotubes and related nanomaterials. Raman experiments of C_{60} peapods were performed by several groups [10, 20–24]. The data are mostly analyzed on the basis of the theoretical predictions stated for individual SWCNTs. The analysis of these experimental results leads to the well-established conclusion: an upshift (downshift) of the peapod radial breathing-like mode (PRBLM) with respect to the RBM of empty SWCNTs occurs for host tube diameters close or smaller (larger) than 1.37 nm [*i.e.*, the diameter of the (10, 10) SWCNT].

Kuzmany et al. [10] have reported a detailed study of the Raman spectra in C_{60} peapods as a function of the temperature and the line excitation. In particular, they estimated the concentration of C_{60} molecules inside the tubes using the measured scattering intensity from the fullerenes relative to that from the tubes. In addition, the absolute concentration of each sample can be evaluated from the Raman measurements (see Table 1 of [10]) because the filling rate of the reference sample was determined from electron energy loss spectroscopy (EELS) to be 60%.

In previous works [11, 25], we studied the different possible configurations of C_{60} molecules inside SWCNTs with diameter lower than 2.15 nm. We predicted that C_{60} molecules inserted inside a SWCNT adopt a linear arrangement for a tube diameter lower than 1.45 nm (called linear peapods) whereas a zigzag configuration is preferred for larger diameters up to 2.15 nm (called zigzag peapods). Raman spectra of free C_{60} peapods and packed in bundles have been calculated for linear and zigzag configurations within the bond-polarizability model [11, 25–27]. Our results were in qualitative agreement with the experiments. In particular, we suggested that (i) the presence of two PRBLMs [22, 23] could be related to a low C_{60} filling rate and (ii) the downshift of the PRBLM in peapods with large diameters could be the fingerprint of the formation of zigzag C_{60} chains [11].

Here, the nonresonant Raman spectra of C_{60} peapods with large diameters (2.15–2.28 nm) are calculated within the framework of the bond-polarizability model combined with the spectral moment's method [28]. This work therefore extends our previous calculations to a larger range of diameters in which C_{60} molecules can adopt a double helix (Figure 1(a)) or a two-molecule layer (Figure 1(b)) configuration [29]. Although the nonresonant approach cannot predict the variation of the line intensities with the excitation energies, our predictions are useful to follow their evolution as a function of different parameters such as the filling rate of C_{60} molecules inside SWCNT. The objectives of our work are threefold. First, we list the ground state configuration of C_{60} molecules inside a nanotube as a function of its diameter. Then, we report for each configuration their associated Raman responses. Finally, we evaluate, for a large range of diameters, the reliability and the transferability of the experimental method proposed by Kuzmany to estimate the relative C_{60} concentration in peapods.

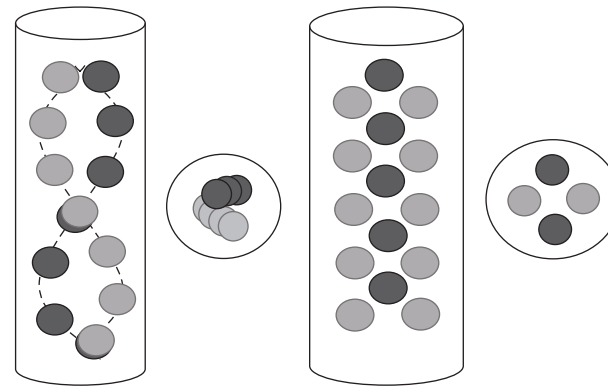

Figure 1: Schematic view of ordered phases resulting from C_{60} packing in single-walled carbon nanotubes: (a) double helix and (b) two-molecule layers.

2. Models and Computational Method

The relaxation of the different structures is obtained from an energy minimization calculation as described in previous works [11].

The dynamical matrix of SWCNT and free C_{60} molecule is calculated using the force constant models parametrized by Saito et al. [30] and Jishi et al. [31], respectively. The dynamical matrices associated with the coupling between the different subsystems (tube-tube, C_{60}-C_{60}, or tube-C_{60}) are described by the usual (12-6) Lennard-Jones potential, $U_{\mathrm{LJ}}(r) = 4\epsilon[(\sigma/r)^{12} - (\sigma/r)^{6}]$, where r is the carbon atom-atom distance. We fixed $\epsilon = 2.964$ meV and $\sigma = 0.3407$ nm according to [12]. This model was successfully used to calculate the generalized phonon density-of-states of C_{60} peapods [32]. We note that similar models were used successfully to model interactions in double-wall carbon nanotubes [24, 33, 34].

The Raman intensities of C_{60} peapods are calculated within the framework of the nonresonant bond-polarizability model [35]. In this model, each bond is characterized by a longitudinal polarizability, α_l, and a polarizability perpendicular to the bond, α_p. Thus, the polarizability contribution of a particular bond b can be written as follows:

$$\alpha_{ij}^{b}(r) = \frac{1}{3}\left(\alpha_l + 2\alpha_p\right)\delta_{ij} + \left(\alpha_l - \alpha_p\right)\left(\widehat{r_i}\widehat{r_j} - \frac{1}{3}\delta_{ij}\right), \quad (1)$$

where i and j are the Cartesian directions (x, y, z) and $\widehat{r}$ is the unit vector along the bond b which connects the atom n and the atom m covalently bonded. The derivatives of (1) with respect to the atomic displacement of the atom n in the direction k, $\pi_{ij,k}^{n}$, are linked to the Raman susceptibility of modes (see [36] for the detailed formalism) and are given by

$$\begin{aligned}\pi_{ij,k}^{n} = \sum_{m}\frac{1}{3}\left(\alpha_l' + 2\alpha_p'\right)\delta_{ij}\widehat{r_k} \\ + \left(\alpha_l' - \alpha_p'\right)\left(\widehat{r_i}\widehat{r_j} - \frac{1}{3}\delta_{ij}\right)\widehat{r_k} \\ + \frac{\alpha_l - \alpha_p}{r}\left(\delta_{ik}\widehat{r_j} + \delta_{jk}\widehat{r_i} - 2\widehat{r_i}\widehat{r_j}\widehat{r_k}\right),\end{aligned} \quad (2)$$

Table 1: Packing parameters obtained from energy minimization of the C_{60} molecules inside SWCNT with several diameters and chiralities.

C_{60} phases	Tube index (n, m)	Tube diameter d_t (nm)	C_{60}-tube distance d_{int} (nm)	C_{60}-C_{60} distance d_m (nm)
Double helix	(22, 9)	2.164	0.321	1.003
	(16, 16)	2.171	0.323	1.001
	(18, 14)	2.176	0.325	0.998
	(25, 5)	2.181	0.323	1.001
	(19, 13)	2.183	0.329	0.998
	(28, 0)	2.193	0.331	1.001
	(27, 2)	2.197	0.312	1.003
	(24, 7)	2.206	0.309	1.003
	(26, 4)	2.210	0.308	1.006
	(22, 10)	2.221	0.30	1.008
Two molecule layers	(28, 1)	2.233	0.312	1.01
	(17, 16)	2.239	0.297	1.002
	(18, 15)	2.242	0.302	1.008
	(19, 14)	2.247	0.308	1.005
	(20, 13)	2.255	0.306	1.006
	(24, 8)	2.259	0.307	1.008
	(21, 12)	2.266	0.311	1.01
	(29, 0)	2.271	0.303	1.007
	(28, 2)	2.276	0.308	1.009
	(22, 11)	2.280	0.310	1.01

where $\alpha' = (\partial\alpha/\partial r)_{r=r_0}$ and r_0 is the equilibrium bond distance. The values of these parameters (α') are usually fitted with respect to the experiments. Here, we use the same set of parameters as the one we used in the Raman calculation of the linear and zigzag C_{60} peapods [11, 26].

3. Results and Discussion

In the framework of the spectral moment's method, Raman frequencies are directly obtained from the position of the Raman lines in the calculated spectra. In all our calculations, the nanotube axis is along the z-axis and a carbon atom is along the x-axis of the nanotube reference frame. The laser beam is kept along the y-axis of the reference frame. We consider that both incident and scattered polarization are along the z-axis to calculate the ZZ-polarized spectra.

3.1. C_{60} Configurations inside Nanotubes. We have previously studied the different possible C_{60} configurations inside SWCNT for diameters (d_t) below 2.15 nm. We found that C_{60} molecules adopt two configurations: linear for $d_t \leq 1.45$ nm and zigzag for $1.45 \leq d_t \leq 2.15$ nm. When the tube diameter increases up to 2.28 nm, the energy minimizations show that two other optimal configurations of C_{60} molecules are possible: a double helix structure ($2.15 \leq d_t \leq 2.23$ nm) and a two-molecule layer ($2.23 \leq d_t \leq 2.28$ nm). Optimized structural parameters issued from the energy minimizations are listed in Table 1.

The optimum diameter of the helix can be obtained as $d_h = d_t - d_m - 2d_{\text{int}}$, where d_m is C_{60} diameter and d_{int} is the interlayer C_{60}-SWCNT distance which can vary from 0.30 to 0.33 nm. These values are consistent with a general interaction for graphitic systems for which the gap distance is 0.33 nm. The double helix can be algebraically described as a single helix [13], whereas for larger tube diameters the structure consists of two-molecule layers with $0.297 < d_{\text{int}} < 0.312$ nm.

For both configurations (double helix and two-molecule layers), the interfullerene C_{60}-C_{60} distance varies from 0.998 to 1.01 nm. This result is in good agreement with the previously reported peapod interball separation of 0.97 nm from electron-diffraction profiles [8] and 0.95 nm from high-resolution transmission electron microscopy (TEM) data [9].

3.2. Raman Spectra of C_{60} Completely Filled Nanotubes. The configuration of the guest molecules inside the nanotube and the Raman spectra of peapods are diameter dependent and do not significantly depend on the tube chirality [11, 27]. Thus, we can restrict our discussion without a loss of generality to zigzag tubes.

Raman spectra of peapods have been calculated for a double helix [C_{60}@(28, 0)] and a two-molecule layer [C_{60}@(29, 0)] configurations of C_{60} molecules. To reach a 100% filling rate, 20 C_{60} molecules have been encapsulated into the (28, 0) SWCNT against 32 C_{60} molecules in the (29, 0) SWCNT. In both configurations, periodic conditions have been used along the tube axis and we considered a tube length of 12.71 nm, leading to a number of carbon atoms close to 3360 in the (28, 0) SWCNT and 3480 in the (29, 0) SWCNT. Thus, the ratio between the number of carbons in C_{60} and the one in the tube, which corresponds to C_{60} concentration in the tubes, is about 36% and 55% for C_{60}@(28, 0) and C_{60}@(29, 0) peapods, respectively. Results are displayed in Figure 2 for the ZZ-polarization and within the PRBLM

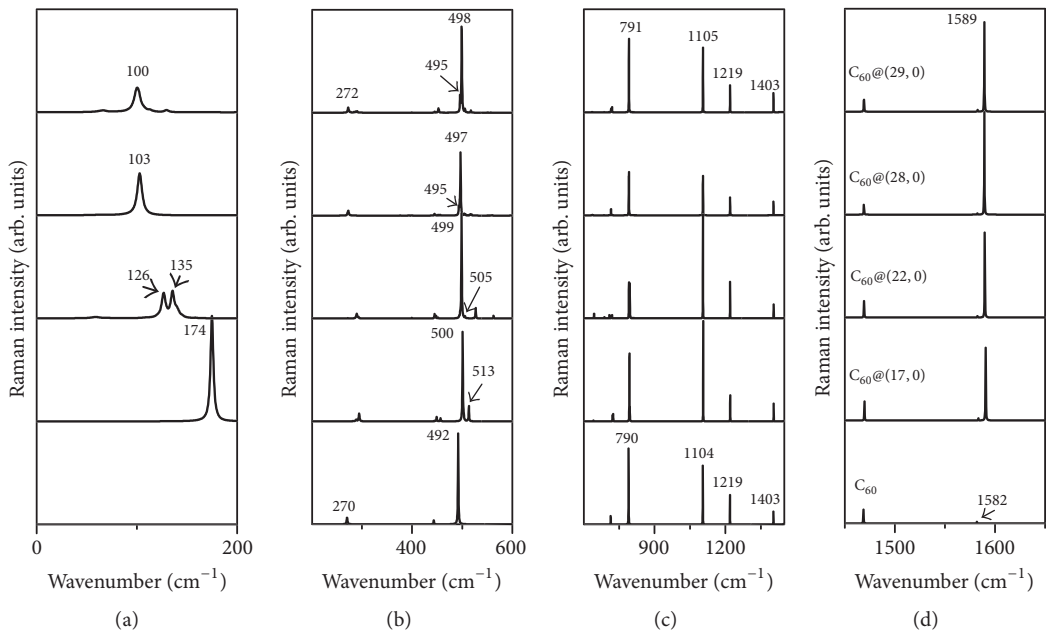

FIGURE 2: Calculated *ZZ*-polarized Raman spectra of C_{60} peapods and free C_{60} molecule.

range (Figure 2(a)), the region of the radial C_{60} modes (Figure 2(b)), the intermediate range (Figure 2(c)), and the range of tangential modes [$A_g(2)$ mode for C_{60} and G-modes for the tubes] (Figure 2(d)). For comparison purposes, we also included in Figure 2 the Raman responses of peapods where C_{60} molecules adopt a linear chain [C_{60}@(17, 0)] and a zigzag chain [C_{60}@(22, 0)], together with a Raman spectrum of a free C_{60} molecule.

For the high-frequency range above 1200 cm^{-1}, the main lines of free C_{60} molecules are located at 1219 ($H_g(6)$), 1403 ($H_g(7)$), 1468 ($A_g(2)$), and 1582 cm^{-1} ($H_g(8)$). These lines are slightly upshifted in peapods by 1-2 cm^{-1} as already reported in linear and zigzag peapods (see Figure 2 in [11]). The tangential-like modes (TLM) in SWCNTs are almost not affected by the insertion of C_{60} molecules inside the nanotube [28].

In contrast, significant changes are observed below 1200 cm^{-1}. In the region of the radial C_{60} modes, $A_g(1)$ line located at 492 cm^{-1} in the free C_{60} spectrum shows a splitting into two components at (500, 513), (499, 505), (495, 497), and (495, 498) cm^{-1} in C_{60}@(17, 0), C_{60}@(22, 0), C_{60}@(28, 0), and C_{60}@(29, 0), respectively. This splitting was also obtained for a model consisting of a single C_{60} molecule capped inside a nanotube, suggesting that it is related to the interactions between C_{60} molecules and the nanotube host, and not to the inter-C_{60} interactions. Below 200 cm^{-1}, the radial breathing mode in (17, 0), (28, 0), and (29, 0) SWCNTs, respectively, located at 168, 102, and 98 cm^{-1}, is upshifted in the corresponding peapods to 174, 103, and 100 cm^{-1}. In C_{60}@(22, 0), the PRBLM displays a double-structure. This feature is made of a low-frequency (high-frequency) component located at 126 cm^{-1} (135 cm^{-1}), downshifted (upshifted) with respect to the position of the RBM located at 129 cm^{-1} in the (22, 0) SWCNT. This shift and splitting depend on the configuration of C_{60} molecules inside SWCNT on one side and on the inter-C_{60} interactions on the other side.

3.3. C_{60} Filling Rate in Nanotubes. In the case of a peapod sample, it seems reasonable to consider that all the nanotubes may not be fully filled with C_{60} molecules. Here, we consider the hypothesis of a partial filling of the tubes with long (quasi-infinite) C_{60} chains. We also assume that the molecules tend to cluster inside nanotubes. Indeed, this should correspond to a low energy configuration of the system as the energy is lowered by the attractive C_{60}-C_{60} interactions. This hypothesis is supported by the observations reported in [37].

Calculated *ZZ*-polarized Raman spectra of C_{60}@(28, 0) (double helix chain of C_{60}) and C_{60}@(29, 0) (two-molecule layer) peapods are reported in Figure 3 as a function of five filling rates (20, 40, 60, 80, and 100%). The TLM range is not reported in this figure because we observed that this range slightly depends on the degree of filling of the SWCNT.

For both C_{60} configurations, a single PRBLM is predicted whatever the tube filling. For the empty tubes, the RBM is located at 102 and 98 cm^{-1} for (28, 0) and (29, 0) SWCNTs, respectively. For a high level of filling, it is upshifted at 103 and 100 cm^{-1} in C_{60}@(28, 0) and C_{60}@(29, 0) peapods, respectively. As expected, the intensity of $H_g(1)$ line located at 270 cm^{-1} in C_{60} increases when the filling factor increases.

At this stage, we investigate the evolution on the ratio between the Raman scattering intensity from C_{60} molecules and that from the tubes as a function of C_{60} concentration inside the tubes. To make the comparison with the experimental results easier, we proceeded into three steps described as follows. (i) We performed an average of the

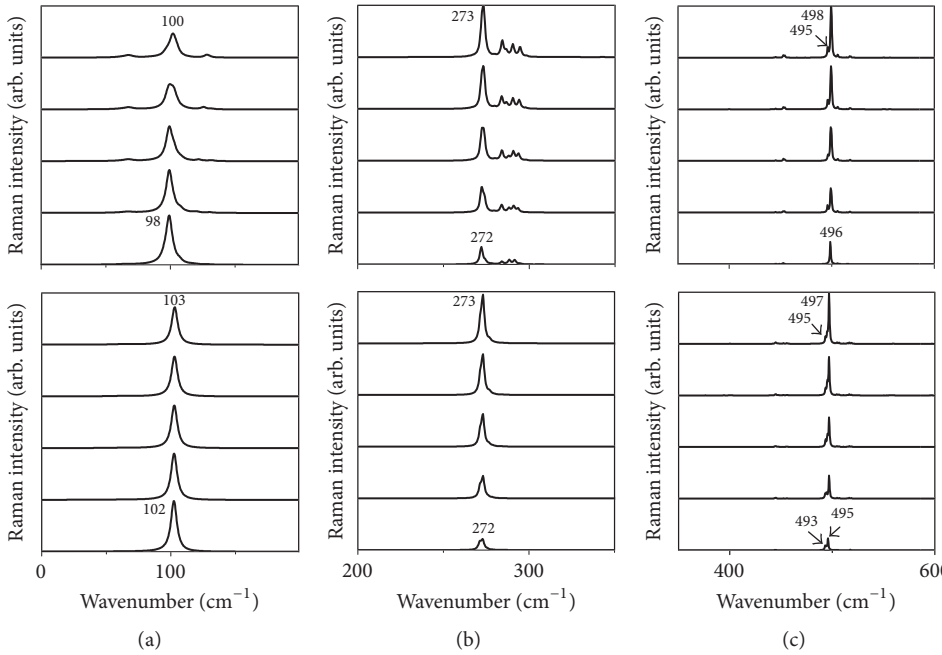

FIGURE 3: Calculated ZZ-polarized Raman spectra of C_{60}@(28, 0) (bottom) and C_{60}@(29, 0) (top) as a function of the filling rate. From bottom to top, the filling rate is 20, 40, 60, 80, and 100%.

Raman spectra over the peapod orientations with regard to the laboratory frame. Raman spectra are calculated in the VV-polarization for unoriented peapod samples. (ii) We calculated the intensity ratio between the Raman lines of C_{60} molecule [$H_g(2)$, $A_g(1)$, $H_g(3)$, $H_g(4)$, $H_g(7)$, and $A_g(2)$] and the PRBLM or G-mode. (iii) We normalized these calculated intensity ratio with respect to the same intensity ratio calculated for the 60% filling factor sample. This normalization was chosen to comply with Kuzmany's choice.

The relative C_{60} concentrations displayed in Figure 4 have been derived according to this procedure for each Raman mode in C_{60}@(17, 0), C_{60}@(22, 0), C_{60}@(28, 0), and C_{60}@(29, 0). These peapods correspond to a configuration where C_{60} molecules adopt a linear, zigzag, double helix, and two-molecule layer orientations, respectively. As expected, for all the investigated peapod diameters, the relative concentrations calculated for each C_{60} mode are close. The relative concentrations calculated for infinite peapods increase when its diameter increases. Indeed, for a filling factor ~20%, the relative concentration is close to 0.21, 0.26, 0.3, and 0.4 for a diameter of 1.35 [C_{60}@(17, 0)], 1.76 [C_{60}@(22, 0)], 2.19 [C_{60}@(28, 0)], and 2.27 nm [C_{60}@(29, 0)], respectively.

Kuzmany et al. [10] performed a detailed Raman analysis of C_{60} concentration in peapod bundles and a host SWCNT of 1.36 nm diameter. In order to compare our results with theirs, we calculated the average intensity ratio, also normalized on the 60% filling rate intensities, between modes of C_{60} in the infinite bundle of C_{60}@(17, 0) and the PRBLM [$H_g(2)$, $A_g(1)$, $H_g(3)$, $H_g(4)$, and $H_g(7)$ mode] or the G-mode of the (17, 0) nanotube [$A_g(2)$]. For a ~70% concentration, the average relative concentrations are found between 0.97 and 1.04 following the different C_{60} phonons modes, in good agreement with the experimental value evaluated [10] ~1.13. For a ~20% concentration (corresponding to the L43 sample (EELS concentration 25 ± 10) in [10]), the average relative concentration is calculated around 0.21 ± 0.02, in good agreement with the experimental relative concentration evaluated around 0.19.

4. Conclusions

In this paper, we investigated on C_{60} peapods for a large range of diameters (2.15–2.28 nm). The optimal configurations of C_{60} molecules are derived using a convenient Lennard-Jones potential. We found that C_{60} molecules adopt a double helix arrangement in SWCNTs with diameters between 2.16 and 2.23 nm, whereas a layer of two molecules is preferred for larger diameters up to 2.28 nm. For the obtained configurations, the nonresonant Raman spectra have been calculated as a function of the tube diameter and C_{60} filling rate using the bond-polarizability model combined with the spectral moment's method. The variation of the average intensity ratio between C_{60} Raman-active modes and the nanotube ones, as a function of the concentration molecules, has been analyzed and a general good agreement is found between calculations and measurements. This good agreement supports the experimental method proposed by Kuzmany et al. to evaluate C_{60} concentration inside SWCNTs.

Finally, to improve the comparison between our models and the experimental data, calculations of the nonresonant Raman spectra of peapods with some structural defects on its wall, as experimentally observed [19, 38], are currently in progress.

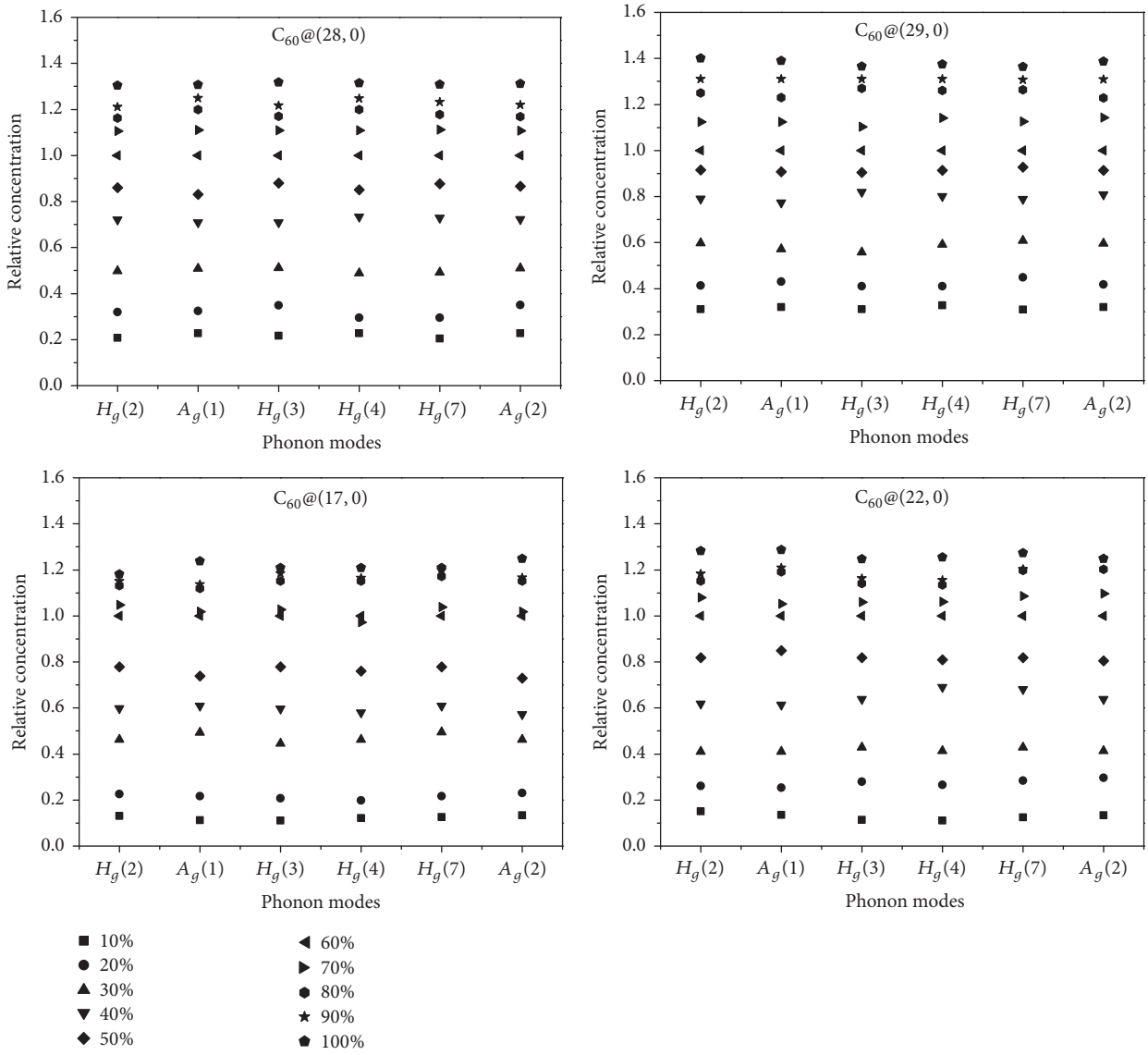

Figure 4: Relative concentration of several configurations of C_{60} inside SWCNTs normalized on the 60% filling rate intensities. The configurations of C_{60} adopt a linear, zigzag, double helix, and two-molecule layer inside (17, 0), (22, 0), (28, 0), and (29, 0), respectively.

Conflicts of Interest

The authors declare that they have no conflicts of interest.

Acknowledgments

Discussions with J.-L. Sauvajol and J.-L. Bantignies from Charles Coulomb Laboratory (University of Montpellier, France) were much appreciated. The work was supported by the University of Moulay Ismail Research Grant (13-2016).

References

[1] B. W. Smith, M. Monthioux, and D. E. Luzzi, "Encapsulated C_{60} in carbon nanotubes," *Nature*, vol. 396, no. 6709, pp. 323-324, 1998.

[2] B. W. Smith, M. Monthioux, and D. E. Luzzi, "Carbon nanotube encapsulated fullerenes: a unique class of hybrid materials," *Chemical Physics Letters*, vol. 315, no. 1-2, pp. 31–36, 1999.

[3] J. Sloan et al., "The size distribution, imaging and obstructing properties of C_{60} and higher fullerenes formed within arc-grown single walled carbon nanotubes," *Chemical Physics Letters*, vol. 316, no. 3, pp. 191–198, 2000.

[4] H. Kataura, Y. Maniwa, T. Kodama et al., "High-yield fullerene encapsulation in single-wall carbon nanotubes," *Synthetic Metals*, vol. 121, no. 1–3, pp. 1195-1196, 2001.

[5] K. Hirahara, K. Suenaga, S. Bandow et al., "One-dimensional metallofullerene crystal generated inside single-walled carbon nanotubes," *Physical Review Letters*, vol. 85, no. 25, pp. 5384–5387, 2000.

[6] R. F. Service, "Nanotube peapods show electrifying promise," *Science*, vol. 292, no. 5514, p. 45, 2001.

[7] Y.-K. Kwon, D. Tománek, and S. Ijima, "'Bucky shuttle' memory device: synthetic approach and molecular dynamics simulations," *Physical Review Letters*, vol. 82, Article ID 1470, 1999.

[8] X. Liu, T. Pichler, M. Knupfer et al., "Filling factors, structural, and electronic properties of C_{60} molecules in single-wall carbon nanotubes," *Physical Review B*, vol. 65, Article ID 045419, 2002.

[9] H. Kataura, Y. Maniwa, T. Kodama et al., "Fullerene-peapods: 619 synthesis, structure, and Raman spectroscopy," *AIP Conference Proceedings*, vol. 591, p. 251, 2001.

[10] H. Kuzmany, R. Pfeiffer, C. Kramberger et al., "Analysis of the concentration of C_{60} fullerenes in single wall carbon nanotubes," *Applied Physics A*, vol. 76, no. 4, p. 449, 2003.

[11] H. Chadli, A. Rahmani, K. Sbai, P. Hermet, S. Rols, and J.-L. Sauvajol, "Calculation of Raman-active modes in linear and zigzag phases of fullerene peapods," *Physical Review B - Condensed Matter and Materials Physics*, vol. 74, no. 20, Article ID 205412, 2006.

[12] H. Ulbricht, G. Moos, and T. Hertel, "Interaction of C_{60} with Carbon Nanotubes and Graphite," *Physical Review Letters*, vol. 90, Article ID 095501, 2003.

[13] M. Hodak and L. A. Girifalco, "Ordered phases of fullerene molecules formed inside carbon nanotubes," *Physical Review B*, vol. 67, Article ID 075419.

[14] M. Hodak and L. A. Girifalco, "Systems of C_{60} molecules inside (10,10) and (15,15) nanotube: a Monte Carlo study," *Physical Review B*, vol. 68, Article ID 085405, 2003.

[15] T. Michel, L. Alvarez, J-L. Sauvajol et al., "Structural selective charge transfer in iodine-doped carbon nanotubes," *Journal of Physics and Chemistry of Solids*, vol. 67, no. 5-6, pp. 1190–1192, 2006.

[16] A. N. Khlobystov, D. A. Britz, A. Ardavan, and G. A. D. Briggs, "Observation of ordered phases of fullerenes in carbon nanotubes," *Physical Review Letters*, vol. 92, no. 24, Article ID 245507, 2004.

[17] F. Simon, H. Peterlik, R. Pfeiffer, J. Bernardi, and H. Kuzmany, "Fullerene release from the inside of carbon nanotubes: a possible route toward drug delivery," *Chemical Physics Letters*, vol. 445, no. 4–6, pp. 288–292, 2007.

[18] V. Zólyomi, H. Peterlik, J. Bernardi et al., "Toward synthesis and characterization of unconventional C66 and C68 fullerenes inside carbon nanotubes," *Journal of Physical Chemistry C*, vol. 118, no. 51, pp. 30260–30268, 2014.

[19] B. W. Smith and D. Luzzi, "Formation mechanism of fullerene peapods and coaxial tubes: a path to large scale synthesis," *Chemical Physics Letters*, vol. 321, no. 1, pp. 169–174.

[20] A. G. Ryabenko, N. A. Kiselev, J. L. Hutchison et al., "Spectral properties of single-walled carbon nanotubes encapsulating fullerenes," *Carbon*, vol. 45, no. 7, pp. 1492–1505, 2007.

[21] S. K. Joung, T. Okazaki, N. Kishi, S. Okada, S. Bandow, and S. Iijima, "Effect of fullerene encapsulation on radial vibrational breathing-mode frequencies of single-wall carbon nanotubes," *Physical Review Letters*, vol. 103, Article ID 027403.

[22] S. Bandow, M. Takizawa, K. Hirahara, M. Yudasaka, and S. Iijima, "Raman scattering study of double-wall carbon nanotubes derived from the chains of fullerenes in single-wall carbon nanotubes," *Chemical Physics Letters*, vol. 337, no. 1–3, pp. 48–54, 2001.

[23] S. Bandow, M. Takizawa, H. Kato, T. Okazaki, H. Shinohara, and S. Iijima, "Smallest limit of tube diameters for encasing of particular fullerenes determined by radial breathing mode Raman scattering," *Chemical Physics Letters*, vol. 347, no. 1–3, pp. 23–28, 2001.

[24] R. Pfeiffer, H. Kuzmany, T. Pichler et al., "Electronic and mechanical coupling between guest and host in carbon peapods," *Physical Review B*, vol. 69, Article ID 035404, 2004.

[25] H. Chadli, A. Rahmani, and J-L. Sauvajol, "Raman spectra of C_{60} dimer and C_{60} polymer confined inside a (10, 10) single-walled carbon nanotube," *Journal of Physics: Condensed Matter*, vol. 22, Article ID 145303, 2010.

[26] H. Chadli, F. Fergani, M. Bentaleb et al., "Influence of packing on the vibrations of homogeneous bundles of C60 peapods," *Physica E: Low-Dimensional Systems and Nanostructures*, vol. 71, pp. 31–38, 2015.

[27] H. Chadli, A. Rahmani, K. Sbai, and J. L. Sauvajol, "Raman active modes in carbon peapods," *Physica A: Statistical Mechanics and its Applications*, vol. 358, no. 1, pp. 226–236, 2005.

[28] A. Rahmani, J-L. Sauvajol, S. Rols, and C. Benoit, "Nonresonant Raman spectrum in infinite and finite single-wall carbon nanotubes," *Physical Review B*, vol. 66, Article ID 125404, 2002.

[29] H. Chadli, F. Fergani, S. A. Ait Abdelkader, A. H. Rahmani, B. Fakrach, and A. Rahmani, "Filling rate dependence on theoritical Raman spectra of carbon C_{60} peapods," *Materials and Devices*, vol. 1, no. 1, p. 1221, 2016.

[30] R. Saito, T. Takeya, T. Kimura, G. Dresselhaus, and M. S. Dresselhaus, "Raman intensity of single-wall carbon nanotubes," *Physical Review B*, vol. 57, Article ID 4145, 1998.

[31] R. A. Jishi, R. M. Mirie, and M. S. Dresselhaus, "Force-constant model for the vibrational modes in C60," *Physical Review B*, vol. 45, no. 23, pp. 13685–13689, 1992.

[32] J. Cambedouzou, V. Pichot, S. Rols et al., "On the diffraction pattern of C60 peapods," *European Physical Journal B*, vol. 42, no. 1, pp. 31–45, 2004.

[33] R. Pfeiffer, C. Kramberger, F. Simon, H. Kuzmany, V. N. Popov, and H. Kataura, "Interaction between concentric tubes in DWCNTs," *European Physical Journal B*, vol. 42, no. 3, pp. 345–350, 2004.

[34] R. Pfeiffer, F. Simon, H. Kuzmany, and V. Popov N, "Fine structure of the radial breathing mode of double-wall carbon nanotubes," *Physical Review B*, vol. 72, Article ID 161404, 2005.

[35] S. Guha, J. Menendez, J. B. Page, and G. B. Adams, "Empirical bond polarizability model for fullerenes," *Physical Review B*, vol. 53, Article ID 13106, 1996.

[36] P. Hermet, N. Izard, A. Rahmani, and P. Ghosez, "Raman scattering in crystalline oligothiophenes: a comparison between density functional theory and bond polarizability model," *Journal of Physical Chemistry B*, vol. 110, no. 49, pp. 24869–24875, 2006.

[37] K. Hirahara, S. Bandow, K. Suenaga et al., "Electron diffraction study of one-dimensional crystals of fullerenes," *Physical Review B*, vol. 64, Article ID 115420, 2001.

[38] B. Burteaux, A. Claye, B. W. Smith, M. Monthioux, D. E. Luzzi, and J. E. Fischer, "Abundance of encapsulated C 60 in single-wall carbon nanotubes," *Chemical Physics Letters*, vol. 310, no. 1-2, pp. 21–24, 1999.